

## Overview of anomalous toroidal momentum transport.

A.G. Peeters<sup>1</sup>, C. Angioni<sup>2</sup>, A. Bortolon<sup>3</sup>, Y. Camenen<sup>4</sup>, F.J. Casson<sup>4</sup>, B. Duval<sup>3</sup>, L. Fiederspiel<sup>3</sup>, W.A. Hornsby<sup>4</sup>, Y. Idomura<sup>5</sup>, N. Kluy<sup>2</sup>, P. Mantica<sup>6</sup>, F.I. Parra,<sup>7</sup> A.P. Snodin<sup>4</sup>, G. Szepesi<sup>4</sup>, D. Strintzi<sup>8</sup>, T.Tala<sup>9</sup>, G. Tardini<sup>2</sup>, P. de Vries<sup>10</sup>, J. Weiland<sup>11</sup>

1 University of Bayreuth, 95440 Bayreuth, Germany

2 Max Planck Institut (IPP) Euratom assoc., Boltzmannstrasse 2 85748 Garching, Germany

3 CRPP-EPFL, Euratom associated, CH-1015 Switzerland

4 University of Warwick, CV7 4AL Coventry, United Kingdom

5 Japan Atomic Energy Agency, Tokyo 110-0015, Japan

6 Istituto di Fisica del Plasma 'P.Caldirola', Associazione Euratom-ENEA-CNR, Milano, Italy

7 Rudolf Peierls Centre for Theoretical Physics, University of Oxford, Oxford, OX1 3NP, UK

8 National Technical University of Athens, (Euratom associated), GR-15773 Athens, Greece

9 Association EURATOM-Tekes, VTT, P.O. Box 1000, FIN-02044 VTT, Finland

10 FOM Institute Rijnhuizen, Association EURATOM-FOM, Nieuwegein, the Netherlands

11 Chalmers University of Technology and Euratom-VR Association, Göteborg Sweden

### Abstract

Toroidal momentum transport mechanisms are reviewed and put in a broader perspective. The generation of a finite momentum flux is closely related with the breaking of symmetry along the field. The symmetry argument allows for the systematic identification of possible transport mechanisms. Those that appear to lowest order in the normalized Larmor radius (the diagonal part, Coriolis pinch, ExB shearing, particle flux, and up-down asymmetric equilibriums) are reasonably well understood. At higher order, thought to be of importance in the plasma edge, the theory is still under development.

### 1. Introduction

Plasma rotation plays a key role in regulating turbulence and has a beneficial effect on energy confinement in fusion devices through ExB shearing [1,2]. Furthermore, a sufficiently large rotation can stabilize the resistive wall mode [3,4]. Toroidal rotation plays a special role in tokamaks due to the symmetry of the device. This symmetry leaves the toroidal angular rotation, in contrast to the poloidal rotation, undamped and, consequently, the toroidal rotation can attain values much in excess of the poloidal rotation. Toroidal velocity shear translates into both ExB shear, perpendicular to the background magnetic field, and parallel velocity shear. While the former is beneficial for confinement, the latter can enhance turbulent transport, since in toroidal geometry the parallel velocity gradient adds a drive to the Ion Temperature Gradient (ITG) mode [5-7]. It is largely the ratio of the poloidal to the toroidal magnetic field strength  $B_p/B_t \approx \epsilon/q$  that determines the relative strength of these two mechanisms. For sufficiently large  $B_p/B_t$  the ExB shear dominates and turbulence is suppressed.

Early experimental observations on momentum transport [8-17] and theoretical investigations into anomalous transport [18] suggest a strong coupling of ion heat and momentum transport, with the diagonal transport coefficients being of similar magnitude. These experiments were performed using neutral beam heating which exerts a large torque on the plasma, and the understanding was that without external momentum input, the plasma rotation would be negligible. This picture radically changed through the discovery of the so-called intrinsic rotation [19-27], i.e. the finite rotation a plasma develops

without an external toroidal torque. The intrinsic rotation is of particular interest to a reactor plasma for which the external torque will be small. Subsequently, mechanisms of toroidal momentum transport have attracted much recent attention in the community, leading to a very rapid development in theory and modelling. This paper will give an overview of the developments in this relatively new area and puts them in a global perspective.

Since toroidal angular momentum is conserved, its evolution equation can be written in conservative form

$$\sum_s \left\{ \frac{\partial m_s n_s R^2 \Omega}{\partial t} \right\} = -\frac{1}{V'} \frac{\partial}{\partial r} \left[ V' \left( \{ \Gamma_\varphi \cdot \nabla r \} + \sum_s \{ m_s R^2 \Omega \Gamma_s \cdot \nabla r \} \right) \right] + \{ S_\varphi \}, \quad (1)$$

where the sum is over all species  $s$ ,  $\Omega(r)$  is the toroidal angular rotation frequency,  $m_s$  ( $n_s$ ) is the particle mass (density),  $R$  is the major radius,  $r$  is the radial coordinate (a flux label),  $V$  is the volume,  $V' = \partial V / \partial r$ ,  $\Gamma_\varphi$  is the toroidal momentum flux,  $\Gamma_s$  is the particle flux,  $S_\varphi$  is the external momentum source, and the brackets  $\{ \}$  denote the flux surface average. The particle flux enters when decomposing the stress

$$\overline{n_s m_s R^2 (\mathbf{v} \cdot \nabla \varphi) (\mathbf{v} \cdot \nabla r)} = \overline{(n_{s0} + \tilde{n}_s) m_s R^2 (\Omega + \tilde{\mathbf{v}} \cdot \nabla \varphi) (\tilde{\mathbf{v}} \cdot \nabla r)} \rightarrow m_s \tilde{n} \tilde{\mathbf{v}}^r R^2 \Omega + m_s n_s R^2 \tilde{\mathbf{v}}^r \tilde{\mathbf{v}}^\varphi, \quad (2)$$

where  $\mathbf{v}$  is the velocity,  $\varphi$  is the toroidal angle, the overline denotes an average over a time interval long compared to the eddy turn over time, and the tilde denotes a fluctuating quantity. Using the expressions of Ref. [28], retaining only the leading term and those quadratic in the potential fluctuations (pressure fluctuations do enter at a similar order [28,29] though) one obtains for the flux surface averaged toroidal momentum flux

$$\Gamma_\varphi^r + \sum_s \{ m_s R^2 \Omega \Gamma_s^r \} = \sum_s \left\{ \frac{R B_t}{B} \int d^3 \mathbf{v} \mathbf{v}_E^r m_s v_\parallel F + R \frac{n_s m_s}{B^2} \frac{\partial \phi}{\partial s} \frac{\partial \phi}{\partial r} + R^2 n_s m_s (\mathbf{v}_E \cdot \nabla \varphi) (\mathbf{v}_E \cdot \nabla r) \right\} \quad (3)$$

where  $B$  is the magnetic field strength,  $\mathbf{v}_E$  is the ExB velocity,  $s$  is the parallel coordinate,  $v_\parallel$  is the parallel velocity,  $\phi$  is the electro-static potential, and  $F$  is the distribution function. The terms in the expression above can be ordered relatively to each other  $1, k_\parallel \rho \approx \rho / R, (k_\perp \rho) (B_p / B)$ , where  $\rho$  is the Larmor radius and  $k_\perp$  is the perpendicular wave vector. The first term in the brackets on the right hand side, i.e. the toroidal component of the parallel momentum flux, therefore, dominates, and we will concentrate on this term in the first part of this paper. Theory must develop an understanding of the fluxes in the equation above. For intrinsic rotation, the interest is in a momentum flux that is not proportional to the rotation gradient.

## 2. Symmetry breaking

Toroidal momentum transport is related to a breaking of symmetry [5,30,31]. As shown in [5,31] a symmetry in the gyro-kinetic equations is found under special limiting circumstances:

1. Lowest order relevant  $\rho_* = \rho / R$  limit. This is often referred to as the local limit. Note that in this limit the parallel velocity nonlinearity does not appear. Also in this limit the turbulence is homogeneous in the plane perpendicular to the magnetic field.
2. Zero toroidal velocity
3. Zero parallel velocity gradient
4. Zero ExB shearing rate (not considered in [5], but evident from the work of [32] )
5. Up-down symmetric equilibrium

The symmetry argument is briefly outlined below. The equation for a perturbed distribution ( $f$ ) is given by

$$\begin{aligned}
\frac{\partial f}{\partial t} + v_{\parallel} \frac{\partial f}{\partial s} + (\mathbf{v}_D + \mathbf{v}_E + \mathbf{v}_{E0}) \cdot \nabla f - \mu \frac{\partial B}{\partial s} \frac{\partial f}{\partial v_{\parallel}} \\
= -\frac{1}{B} \frac{\partial \langle \phi \rangle}{\partial y} \left[ \frac{1}{L_n} + \left( \frac{mv^2}{T} - \frac{3}{2} \right) \frac{1}{L_T} - \frac{m(v_{\parallel} - RB_t \Omega / B) RB_t \nabla \Omega}{T B} \right] F_M \\
- \left( v_{\parallel} \frac{\partial \langle \phi \rangle}{\partial s} + \mathbf{v}_D \cdot \nabla [\langle \phi \rangle + \Phi] \right) \frac{Ze}{T} F_M,
\end{aligned} \tag{4}$$

where field aligned coordinates  $(r, y, s)$  are used with  $y$  the binormal coordinate. The parallel velocity and magnetic moment ( $\mu$ ) are used as velocity space coordinates,  $\mathbf{v}_D$  is the drift due to the inhomogeneous magnetic field,  $\mathbf{v}_E = \mathbf{b} \times \nabla \langle \phi \rangle / B$  ( $\mathbf{v}_{E0}$ ) is the ExB drift due to fluctuating (background) potential  $\langle \phi(r, y) \rangle$  ( $\Phi(r)$ ), and  $F_M$  is the Maxwell distribution shifted in the parallel velocity direction by the mean velocity  $RB_t \Omega / B$ . The gradients of density and temperature are represented by  $1/L_n \equiv -\nabla n / n$  and  $1/L_T \equiv -\nabla T / T$ . The equation above is derived for a toroidally rotating plasma. Diamagnetic and neo-classical equilibrium effects are neglected in agreement with the lowest order  $\rho_*$  approximation. Note too that the magnetic field strength  $B$  appears instead of  $B^*$ , again in agreement with  $\rho_* \ll 1$ .

A transformation is constructed for which the parallel momentum flux changes sign, leaving the gyro-kinetic equation invariant. The former is obtained through a change in the sign of the parallel velocity, i.e.  $v_{\parallel} \rightarrow -v_{\parallel}$ . From the parallel streaming term (second term in the equation above) it is clear that to leave the equation invariant also the coordinate along the field line must change sign  $s \rightarrow -s$ . This also leaves the fourth term on the left hand side invariant. However, the terms on the right hand side are invariant only if  $F_M$  is even in the parallel velocity, i.e. the equilibrium does not have a net parallel flow [condition 2], and the gradient in the parallel velocity is zero [condition 3]. Turning to the drift due to the magnetic field inhomogeneity: In the local limit the drift depends only on the coordinate along the field line

$$\mathbf{v}_D \cdot \nabla = D^y(s) \frac{\partial}{\partial y} + D^r(s) \frac{\partial}{\partial r} \tag{5}$$

The equation is invariant if  $D^y(s) = D^y(-s)$  which is true for a magnetic equilibrium that is up-down symmetric [condition 5]. However, even for an up-down symmetric equilibrium, the radial component of a vertical drift changes sign when going from the lower to the upper half of the equilibrium, i.e.  $D^r(s) = -D^r(-s)$ . The equation can be made invariant only through the transformation  $r \rightarrow -r$ . The latter transformation requires that the background ExB velocity is even in  $r$ , and hence there is no ExB shearing [condition 4]. Furthermore, the Maxwellian background must be even in  $r$ , which is satisfied in the local limit [condition 1]. With these transformations, the linear equation is invariant [5], but the nonlinear term still changes sign

$$\mathbf{v}_E \cdot \nabla = \frac{\partial \langle \phi \rangle}{\partial r} \frac{\partial}{\partial y} - \frac{\partial \langle \phi \rangle}{\partial y} \frac{\partial}{\partial r} \tag{6}$$

The transformation [31]  $f \rightarrow -f$  and  $\phi \rightarrow -\phi$  changes the sign of all the linear terms, but leaves the nonlinear terms unchanged. Multiplying the original equation with -1, the set of transformations can then be seen to leave the equation invariant. The procedure has been outlined here for the electro-static collisionless case without considering the field equations. The extension to the electro-magnetic case with collisions, as well as the analysis of the field equations is, however, straight forward. In conclusion the gyro-kinetic  $\delta f$  equation is invariant under the transformation

$$v_{\parallel} \rightarrow -v_{\parallel} \quad s \rightarrow -s \quad r \rightarrow -r \quad f \rightarrow -f \quad \phi \rightarrow -\phi \quad \delta A_{\parallel} \rightarrow \delta A_{\parallel} \quad \delta B_{\parallel} \rightarrow -\delta B_{\parallel} \tag{7}$$

provided the five condition mentioned at the beginning of the section are satisfied. If  $[f(r, y, s, v_{\parallel}, \mu, t), \phi(r, y, s), \delta A_{\parallel}(r, y, s), \delta B_{\perp}(r, y, s)]$  is a solution of the gyro-kinetic equation, then

$[-f(-r, y, -s, -v_{\parallel}, \mu, t), -\phi(-r, y, -s), \delta A_{\parallel}(-r, y, -s), -\delta B_{\parallel}(-r, y, -s)]$  satisfies the equation as well. Linearly they would grow with equal growth rate, and nonlinearly both solutions would occur with equal probability. The toroidal component of the radial parallel momentum flux ( $\Gamma_{\parallel}^r$ )

$$\Gamma_{\parallel}^r = - \sum_s \left\{ \frac{RB_t}{B} \int d^3\mathbf{v} \frac{1}{B} \frac{\partial}{\partial y} [\langle \phi \rangle - v_{\parallel} \langle \delta A_{\parallel} \rangle + \mu \langle \delta B_{\parallel} \rangle] m_s v_{\parallel} f_s \right\} \quad (8)$$

of both solutions, however, has the opposite sign, and it follows that the net momentum flux is zero. In the nonlinear state this statement is of course only satisfied in a statistical sense.

In linear theory, for the most unstable mode, the symmetry described above comes out directly through the symmetry of the linear mode, i.e.  $f(r, y, s, v_{\parallel}, \mu, t) = f(-r, y, -s, -v_{\parallel}, \mu, t)$  as shown in top panel of Fig. 1 (for parameters see Ref. [33]). The potential is then symmetric in the midplane while the parallel velocity fluctuations are anti-symmetric. This yields zero net parallel momentum transport when integrating over the flux surface, with the flux generated at the top half of the torus being compensated by the bottom half.

The symmetry property is a powerful tool in interpreting the momentum flux. First it has a direct consequence for the toroidal momentum flux in that there are no direct contributions to the flux driven by the density and temperature gradients. These gradients do not result in a breaking of the symmetry in the local limit. Second it allows for a systematic identification of the mechanisms that can drive momentum transport. All must be connected with violating one or more of the constraints mentioned at the beginning of this section. Indeed it has been found that a violation of each of the conditions given above can generate a momentum flux, although it must be stated that the breaking of symmetry is a necessary but not a sufficient condition.

If the terms that break the symmetry are sufficiently small one can do a perturbation theory and arrive at a linear expression for the ion momentum flux (electrons are ignored here due to their small mass)

$$\Gamma_{\phi}^N = \chi_{\phi}^N u' + V_{\phi}^N u + M_{\phi}^N \gamma_E + C_{FS}^N + \rho_* C_*^N \quad (10)$$

Here and in the remainder of this paper normalized quantities are used

$$\Gamma_{\phi}^N = \frac{\Gamma_{\phi i}}{m_i n_i R \rho_*^2 v_{thi}^2} \quad u' \equiv -\frac{R^2 \nabla \Omega}{v_{thi}} \quad u = \frac{R \Omega}{v_{thi}} \quad \gamma_E = \frac{R}{v_{thi}} \frac{(RB_p)^2}{B} \frac{\partial^2 \Phi}{\partial \psi^2}$$

$$\left( \chi_{\phi}^N, V_{\phi}^N, M_{\phi}^N \right) = \frac{(\chi_{\phi}, RV_{\phi}, M_{\phi})}{\rho_i^2 v_{thi} / R} \quad C_{FS}^N + \rho_* C_*^N = \frac{\Gamma_{\phi FS} + \Gamma_{\phi*}}{m_i n_i R \rho_*^2 v_{thi}^2} \quad (11)$$

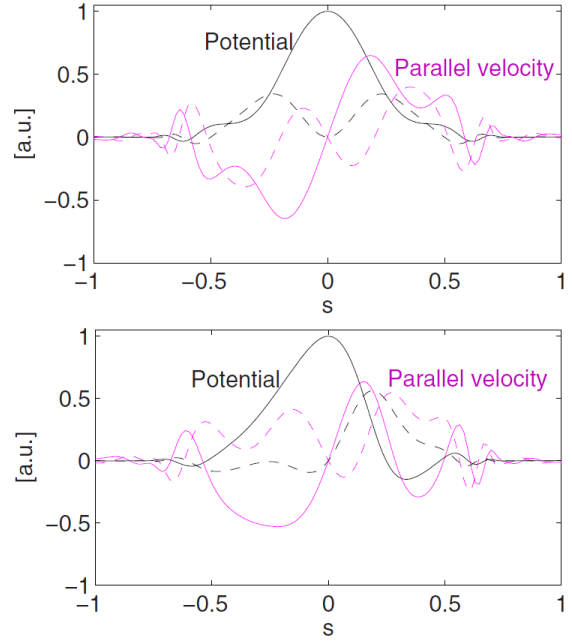


Figure 1 (From Ref. [33]) Linear mode structure along the field line: Potential (black) and the parallel velocity (pink). The real part of the eigenfunction is given by the solid line while the dashed line gives the imaginary part.  $s = \theta/2\pi = -1, 0, 1$  corresponds to the low field side, while  $s = -0.5, 0.5$  corresponds to the high field side. (Calculated with GKW [34])

where  $\psi$  is the poloidal flux, and  $v_{thi} = \sqrt{2T_i/m_i}$  is the thermal velocity of the ions. Note that the diagonal part is defined using the gradient of the angular rotation  $\Omega$  and not with the gradient of the toroidal rotation velocity. Using the normalizations above  $u$  is the toroidal Mach number. The toroidal momentum flux consists of various contributions: the first term is the diagonal contribution (i.e. proportional to  $u'$ ), the second is the Coriolis pinch (proportional to  $u$ ), the third is due to the ExB shearing (proportional to  $\gamma_E$ ), the fourth is the effect of an up-down asymmetric equilibrium, and the fifth is the collection of all effects that require a higher order  $\rho_*$  term in the gyro-kinetic equation. The latter term is naturally  $\rho_*$  smaller compared with the first four, which is explicitly denoted by taking  $\rho_*$  out of the coefficient. Below, unless explicitly denoted otherwise, the quantities are normalized and the index N will be dropped. When the perturbation theory applies, all coefficients ( $\chi_\phi, V_\phi, M_\phi, C_{FS}, C_*$ ) are independent of the symmetry breaking terms ( $u', u, \gamma_E, \dots$ ). This linear form is reasonably well satisfied for the diffusion and pinch under experimental relevant conditions since the instabilities are dominantly driven by the density and temperature gradients. The ExB shear, however, shows a relatively strong nonlinear behaviour [35,36], and leads to the suppression of turbulence, i.e. reduces all the transport coefficients. Finally the shearing rate is related to the toroidal velocity shear. Using the radial force balance and the neo-classical expression for the poloidal rotation  $V_\theta = \alpha \nabla T / eB$ , where  $\alpha$  is of order unity and depends on the collisionality regime, one arrives at

$$\gamma_E = \frac{B_p}{B_t} u' - \frac{1}{2} \rho_* \left[ \frac{R^2 d^2 n}{n dr^2} + (1 - \alpha) \frac{R^2 d^2 T}{T dr^2} + 2 \frac{R^2 dn dT}{nT dr dr} \right], \quad (12)$$

where derivatives of the magnetic components have been neglected against the profile derivatives. Through the dependence of  $\gamma_E$  on  $u'$  the ExB shearing acts as a correction to the diagonal part of the momentum flux. The second term on the right hand side is independent of the toroidal rotation or its gradient, and is one order smaller in  $\rho_*$ . One might be tempted to consider the  $\rho_*$  terms in the toroidal momentum equation small under all circumstances. This is not necessarily justified. The expression for  $\gamma_E$  for instance depends on the second derivative of the density and temperature profiles. Adopting  $(R/L_T)^2$ , as a simple estimate for the term in the square brackets, one recognises that the parameter in front of  $\rho_*$  varies from roughly 40 in the core to values larger than 1000 in the edge. While the ExB shearing can therefore be expected to be relatively small in the core under most conditions, this statement is certainly not true for the edge of the plasma where it could dominate the momentum flux.

In conclusion the momentum flux in the core of a large machine can be expected to be described by

$$\Gamma_\phi = \left( \chi_\phi + \frac{B_p}{B} M_\phi \right) u' + V_\phi u + \text{Order}[\rho_* M_\phi (R/L_T)^2] \quad (13)$$

where the up-down asymmetry term and the particle flux have not been included since they are found to be small in the core (see below). This equation can also be understood to define a high flow regime. Assuming  $V_\phi \approx M_\phi$  (which is indeed roughly satisfied see below), one obtains

$$\text{High flow regime : } u > \rho_* (R/L_T)^2 \quad (14)$$

In the high flow regime higher order correction in  $\rho_*$  can be neglected. Note that high flow here does not mean a Mach number close to 1. For experiments with neutral beam heating  $u = 0.1-0.3$ , typically, and the high flow regime often applies. Interestingly, some spontaneous rotation experiments develop a healthy toroidal velocity with  $u$  reaching values up to 0.2 (See Fig. 2 of Ref. [26]), but there are intrinsic rotation experiments for which the low flow ordering is more appropriate. For turbulence suppression it is the high flow case that is of importance. Using the Waltz rule [2], estimating the growth rate to be

$$\gamma^N = \frac{R\gamma}{v_{thi}} = \beta \left( \frac{R}{L_T} - \frac{R}{L_{Tcrit}} \right) \rightarrow u = \beta \frac{B}{B_p} \left( 1 - \frac{L_T}{L_{Tcrit}} \right) \quad (15)$$

where  $\beta$  is a dimensionless quantity of order unity, and a similar gradient length for the rotation as for the temperature gradient  $u' = R/L_T u$  is assumed. With  $\beta = 0.2$  and  $B/B_p = 10$  typically, it is clear that a substantially smaller  $L_T$  compared with  $L_{Tcrit}$  requires  $u = O(1)$ . The case for the stabilization of the resistive wall mode appears similar, though less severe, since a rotation  $u = 0.1$  is predicted to be necessary to stabilize this mode [37]

Note that the expression of the momentum flux in the high flow regime has a trivial solution  $u = 0$ . To develop a finite plasma rotation a residual stress, i.e. a momentum flux independent of the rotation or its gradient, is necessary. For a large tokamak this mechanism would be expected to be active in the plasma edge. Once a seed rotation is provided, the pinch, as well as a possible reduction in the diagonal part due to the ExB shearing, will enhance the gradient of the rotation in the core of the plasma.

### 3. Contributions to the momentum flux

#### 3.1 The diagonal contribution.

A finite radial gradient in the angular frequency leads to a diagonal (diffusive) contribution. Early work based on fluid models already established a strong coupling between ion heat and momentum transport [18]. This coupling is expressed in the dimensionless Prandtl number (Pr) which is the ratio of the momentum and ion heat diffusivities  $Pr = \chi_\phi / \chi_i$ . The Prandtl number has more recently been assessed through linear [5,38,39], and nonlinear gyrokinetic simulations using adiabatic electrons [40,41] as well as with full electron dynamics [35,42,43] confirming a Prandtl number of order unity. The values reported however cover a range 0.24 - 1.2. This is in itself not entirely surprising since the values have been obtained for different plasma parameters, and the Prandtl number is not a universal constant. Nevertheless, flux tube simulations [44] yield a relatively weak dependence on plasma parameters, and therefore suggest that part of the range could be related to additional momentum transport mechanisms. In global simulations, for instance, finite  $\rho_*$  effects can enter, and for a purely toroidally rotating plasma the toroidal velocity shear is connected with an ExB shear which drives an additional flux. Furthermore, for global simulations large scale long lived zonal flows have been observed to influence the momentum flux [43]. These effects have not always been corrected for in the determination of the Prandtl number, perhaps explaining part of the range observed.

#### 3.2 The Coriolis pinch effect.

The symmetry is also broken for a toroidally rotating plasma, leading to a momentum pinch [45,46]. In the local limit, the effect can be elegantly derived by transforming to the reference frame that moves with the plasma [45]. In this frame the plasma rotation is naturally zero, and enters the physics description only through the Coriolis and centrifugal forces. It is the Coriolis force ( $\mathbf{F}_{co}$ ) that is of main interest in the generation of momentum transport [47] and the centrifugal force will be neglected below. In a magnetised plasma this force generates a Coriolis drift velocity [48,45]

$$\mathbf{F}_{co} = 2m v_{\parallel} \mathbf{b} \times \boldsymbol{\Omega} \rightarrow \mathbf{v}_{co} = \frac{2mv_{\parallel}}{ZeB} \boldsymbol{\Omega}_{\perp} \quad (16)$$

The plasma rotation then enters the gyro-kinetic equation only through this additional drift

$$\frac{\partial f}{\partial t} + \frac{2mv_{\parallel}}{ZeB} \boldsymbol{\Omega}_{\perp} \cdot \nabla f + \dots = \dots - \frac{2mv_{\parallel}}{ZeB} \boldsymbol{\Omega}_{\perp} \cdot \nabla \langle \phi \rangle \frac{Ze}{T} F_M. \quad (17)$$

which appears as a convection as well as an addition particle acceleration due to the drift in the gradient of the perturbed potential. Unlike the other drifts, the Coriolis drift velocity is linear in the parallel

velocity. When building moments of the gyro-kinetic equation, the drift due to the inhomogeneous magnetic field can be seen to couple the even moments of the distribution (density, temperature), but not even with odd moments. The Coriolis pinch, however, does, such that in its presence density and temperature perturbations over the convection term generate parallel velocity fluctuations. These are then transported by the ExB velocity, leading to a finite flux of parallel momentum. The second effect is due to the change in the parallel velocity due to the acceleration in the fluctuating potential. For an ITG with adiabatic electrons the two contributions lead to an inward pinch [45,33]. A fluid model yields

$$\frac{V_\phi}{\chi_\phi} = -4 - \frac{R}{L_N} \quad (18)$$

The Coriolis pinch effect then enhances the central rotation, independent of the rotation direction.

The Coriolis pinch is present also in the laboratory frame, although it must obviously manifests itself differently. The theory in the Laboratory frame has been worked out in Ref. [46], where the two contributions mentioned above have been identified as thermoelectric and ExB compression. The theories of the co-moving and laboratory frame have been shown to be equivalent in Ref. [49]. The ExB compression effect can in the nonlinear regime also be described with the theory of Turbulence Equipartition [50,51].

The study of the Coriolis pinch effect has also revealed that the breaking of symmetry is a necessary, but not a sufficient condition [33]. This is shown in the lower panel of Fig. 1. A linear gyro-kinetic calculation with adiabatic electrons reveals an asymmetric mode structure, but potential and parallel velocity fluctuations nevertheless arrange themselves to yield a zero momentum flux. This process is confirmed by nonlinear simulations (see Ref. [33]), and results from a finite parallel wave vector that exactly compensates the Coriolis drift effect. A finite Coriolis pinch requires the inclusion of kinetic electrons, which due to their trapping can prevent complete cancellation between the Coriolis drift effect and the parallel wave vector of the eigenmode. This leads to the counter intuitive result that the Coriolis pinch scales with the trapped electron fraction, i.e.  $\sqrt{\epsilon}$ . It also explains the poor performance of the fluid models in which kinetic electrons are not accounted for, like Eq. (18) above, which generally over predict the momentum pinch by roughly a factor 2.

Parameter dependences of the pinch from linear gyro-kinetic simulations are shown in Fig. 2. Similar to the fluid model, the density gradient leads to an enhancement of the pinch. The Coriolis drift is in the vertical direction, and similar to the curvature drift, the mode needs to be localized on the outboard side of the surface for it to have an effect. A reduction in the Coriolis pinch is therefore observed when the mode is less localized. This explains the decrease of the pinch with the perpendicular wave vector, the magnetic shear and the safety factor. It is to be noted that all these dependencies mean that the pinch effect is expected to decrease towards the core of the plasma where the safety factor, magnetic shear, trapped

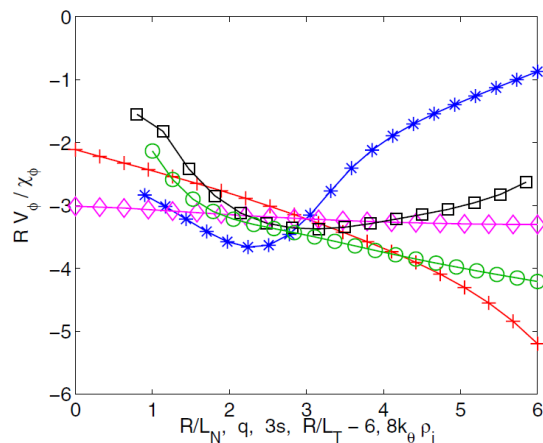


Figure 2 (From Ref. [45]) parameter dependence of the Coriolis pinch from linear gyro-kinetic simulations (GA-STD [2] case) as a function of  $R/L_N$  (+), magnetic shear  $3\hat{s}$  (\*), safety factor (o), temperature gradient (diamond), and poloidal wave vector  $8k_y\rho_i$  (square)

particle fraction and density gradient are smaller. A pinch effect is also observed for the Trapped Electron Mode (TEM) [52], although the pinch effect is smaller in this case.

### 3.3 The particle flux effect.

The particle flux appears in the equation for the toroidal angular momentum conservation. Essentially, one can think of the particles carrying their individual momentum with them when they move radially outward. Knowledge of the particle flux, which is well studied [53-56], directly allows for an evaluation of this contribution. Under stationary conditions with central Neutral Beam heating (NBI) the particle flux is outward and will reduce the total plasma angular momentum. Note that this mechanism, like the diagonal part and the Coriolis pinch, is not able to provide a seed rotation, since the flux of momentum is proportional to the background rotation. Due to the small particle fuelling, the particle flux under will be relatively small under experimental relevant conditions. For NBI heated plasmas  $Q = E \Gamma$ , where  $Q$  is the heat flux and  $E$  is the energy of the injected particles, one can estimate the ratio of the particle flux term against the diagonal contribution

$$\frac{m_i R^2 \Omega \Gamma}{m_i n_i \chi_\phi R^2 \nabla \Omega} = \frac{\Gamma L_\Omega}{n_i \chi_\phi} \approx \frac{\Gamma L_\Omega \nabla T}{Q_i} = \frac{L_\Omega T}{L_T E} \quad (19)$$

where  $L_\Omega = -\Omega / \nabla \Omega$ , and in the second step  $\chi_\phi \approx \chi_i$  and  $Q \approx Q_i = n \chi_i \nabla T$  have been used. Since  $T/E \ll 1$  the particle flux term is usually only a few per cent compared the diagonal contribution. Of course, in the edge of the plasma the influx of neutrals might enhance the effect, and it could possibly be important.

### 3.4 ExB shearing

Background ExB shearing breaks the  $r \rightarrow -r$  symmetry and can induce a flux of toroidal momentum [32,57,58,35,36]. Note that this symmetry breaking induces an asymmetric parallel mode structure. The process can, in simple terms, be understood as follows. The shearing rotates the eddy structures increasing

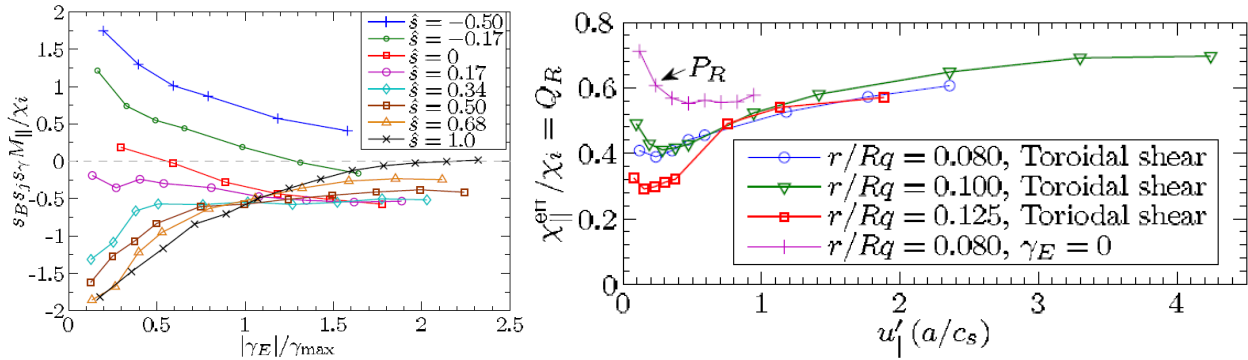


Figure 3 (From Ref. [36]) Left: Ratio of the transport coefficients  $M_\phi / \chi_i$ . Right: effective Prandtl number as a function of the parallel velocity gradient with the ExB shear adjusted to have a purely sheared toroidal rotation, i.e. with zero poloidal rotation

the perpendicular wave number which leads to stabilization of the mode. However, the magnetic field also has a shear and the mode can ‘escape’ the rotational shear by moving along the field such that the magnetic shear undoes the ExB shear. It thereby shifts the position of maximum wave amplitude away from the low field side leading to an asymmetry in the parallel mode structure. Indeed the momentum flux changes sign with the sign reversal of the magnetic shear [57,58,36], although the result is not exact, i.e.

symmetry breaking persists at zero magnetic shear, due to another subsidiary effect causing the asymmetry in the parallel mode structure.

The effect of ExB shearing has been studied through nonlinear gyro-kinetic simulations. The ratio of the coefficients  $M_\phi / \chi_i$  is shown in the left panel of Fig. 3 as a function of the ExB shearing rate normalized to the maximum growth rate of the modes, for various values of the magnetic shear. The ratio  $M_\phi / \chi_i$  is of order unity confirming (part of) the scaling discussed earlier. For small shearing rates  $\gamma_E \ll \gamma_{max}$  the ratio  $M_\phi / \chi_i$  is independent of  $\gamma_E$ , but at larger  $\gamma_E$ ,  $M_\phi / \chi_i$  decreases with  $\gamma_E$ . This is not due to the familiar ExB shear stabilization, since the ratio is insensitive to the turbulence level. The result of Fig. 3 rather shows that momentum transport due to ExB shearing becomes less efficient when background ExB shearing strongly stabilizes the transport. This nonlinear effect might complicate the interpretation of the edge of H-mode experiments where ExB shearing is strong. For  $\gamma_E \approx \gamma_{max}$ , the ratio  $M_\phi / \chi_i$ , furthermore becomes a function of  $u'$  [36] and it appears that cases of strong ExB shearing require nonlinear simulations to assess the momentum flux.

The ExB shear connected with the radial gradient in the toroidal velocity acts as a correction to the diagonal contribution of the momentum flux. Fig. 3 (right) shows the ‘total momentum diffusivity’

$$\chi_\phi^{tot} = \left( \chi_\phi + \frac{B_p}{B} M_\phi \right) \quad (20)$$

normalised to the ion heat conductivity as a function of  $u'$ . The different curves are for different values of  $B_p/B = r/qR$ . For a sufficiently positive magnetic shear, the ExB shearing contribution always reduced the Prandtl number independent of the sign of the magnetic field or plasma current. The decrease can be quite substantial with values as low as  $\chi_\phi^{tot} = 0.3$  being reached. At larger values of  $u'$  and, consequently, larger values of  $\gamma_E$  the reduced efficiency of the ExB shear in driving momentum transport means that the various curves approach each other.

### 3.5 Up-down asymmetric equilibrium

An up-down asymmetric equilibrium naturally breaks the symmetry along the magnetic field and a finite flux of toroidal momentum results [59, 60]. In principle this symmetry breaking is connected with all the geometry quantities, but studies have revealed that the asymmetry in the curvature operator and perpendicular wave vector generate 80% of the effect. A significant flux is only obtained if the extension of the mode along the field is large enough to ‘feel’ the asymmetry. Consequently, a maximum in the flux is often obtained for a relatively long wave length  $k_\perp \rho \approx 0.15$ . The complex interplay between the asymmetry of the equilibrium and the localization of the mode has so far prevented the development of a simple scaling formula to quantify, or even to determine the sign of, the momentum flux. For a given case, the momentum flux changes sign when the sign the magnetic field or plasma current is changed, or when the equilibrium is flipped upside down.

Unlike the other leading  $\rho_*$  effects, the up-down asymmetry generates a flux that is

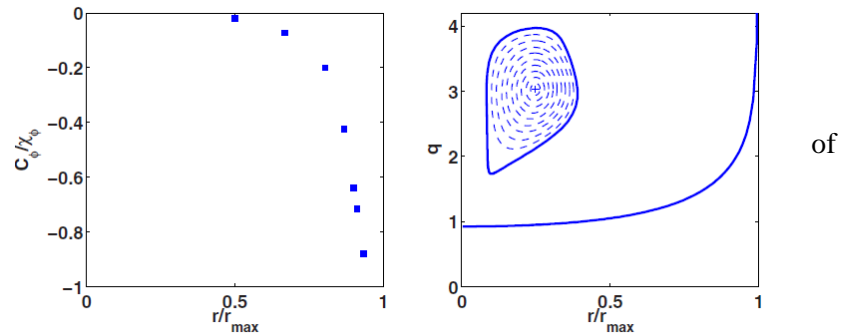


Figure 4 (From Ref. [59]) Left: the ratio of the coefficients  $C_{FS}/\chi_\phi$  as a function of radius. Right: the equilibrium used and the safety factor profile as a function of radius.

independent of the rotation or its gradient, i.e. it can provide a seed rotation. Its magnitude depends on the magnitude of the asymmetry which is found to strongly decay when moving closer to the magnetic axis. Consequently, the effect is largest at the plasma edge as shown in Fig. 4. For the equilibrium, shown in the second panel of Fig. 4, the ratio of the coefficients  $C_{FS}/\chi_\phi$  reaches unity close to the edge. When integrated over the whole profile it predicts a core rotation of  $u = 0.05$  (without considering any other mechanism that could further enhance the rotation of the core).

### 3.6 Higher order $\rho_*$ terms.

So far, the local limit or lowest order  $\rho_*$  approximation has been discussed. In higher order many different effects can break the symmetry. Or, perhaps better stated, there is no symmetry. The theory in this area is still under development and it appears that not all possible mechanisms have been explored. Known symmetry breaking mechanisms include: a radial profile variation of the turbulent amplitude (or more correctly the turbulent wave quanta density) [30], the parallel velocity nonlinearity (or polarization drift) [61,62], ExB shearing due to the pressure gradient contribution to the radial electric field [63], and neo-classical effects [28].

The parallel velocity nonlinearity enters the gyro-kinetic equation in higher order in  $\rho_*$ .

$$\frac{\partial f}{\partial t} + \dots - \frac{Ze}{m} \frac{\partial \langle \phi \rangle}{\partial s} \frac{\partial f}{\partial v_\parallel} - v_\parallel \frac{\mathbf{b} \times (\mathbf{b} \cdot \nabla) \mathbf{b}}{B} \cdot \nabla \langle \phi \rangle \frac{\partial f}{\partial v_\parallel} = \dots \quad (21)$$

For the symmetry to hold, all terms in the gyro-kinetic equation must change sign under the general transformation of Eq. (7). It is clear, however, that the velocity nonlinearity does not and, consequently, can be expected to drive a toroidal momentum flux. Furthermore, the derivation of the momentum theorem for the full  $f$  gyro-kinetic equation shows that the second term on the right hand side of Eq. (3) is related to the velocity nonlinearity in the gyro-kinetic equation. (The  $\delta f$  formalism discussed so far does not have an exact momentum conservation theorem. For full  $f$  gyro-kinetics see [28,29,64]). Applying the symmetry argument to this equation both the first and the third term vanish, but not the second. The parallel velocity nonlinearity, therefore, can act both through the second term in the equation above as well as through the higher order non-symmetric part of  $f$ . It has been shown [61] to generate a momentum flux comparable in magnitude to the ExB shearing connected with the pressure gradient contribution.

An interesting new development is the coupling of turbulence and neo-classical effects [28]. The neo-classical correction to the distribution function is of order  $(B/B_p)\rho_*(R/L_N)$  and therefore need not be kept in the lowest order  $\rho_*$  description. In next order it, however, appears and since the correction contains plasma flows along the magnetic field, it generates a momentum flux. This flux is expected to be larger by a factor  $B/B_p \approx 10$  compared to the turbulent induced fluxes and would then provide the dominant contribution to the momentum flux. An analytic treatment has shown [28] that in order to calculate this effect one needs to solve only the lowest order turbulence equation, i.e. the equation of the local limit, with the background distribution modified to include the neo-classical equilibrium.

For all finite  $\rho_*$  effects, an accurate assessment of the magnitude of the fluxes through numerical simulations is still lacking. Such simulations appear to be necessary to ultimately decide which of the effects is dominant under what conditions.

## 5. Conclusions

Significant progress is made in recent years on the understanding of momentum transport in tokamak plasmas. The lowest order  $\rho_*$  effects have been identified, and through the symmetry argument we know

there are no other contributions at this order than the ones identified. A rough idea of their magnitude exists, and for some of the effects their interplay has been analysed. There is however a need for further exploration. The interplay between the various symmetry breaking mechanisms is insufficiently well understood. Determining the transport coefficients in a larger parameter range might perhaps not increase our physical insight further, but will help us to better understand how the theory matches experimental observations. Furthermore, electro-magnetic effects and instabilities other than the ITG have hardly been touched upon. For the plasma core, linear calculations reveal that electro-magnetic effects might have an impact on the Prandtl number [38]. For the plasma edge the impact of electro-magnetic effects is expected to be significant [65]. The trapped electron mode has been studied in Refs. [30,52], but certainly requires further study.

The situation is less clear for the momentum transport to higher order in  $\rho_*$ . Understanding these transport contributions is essential for the understanding of the edge as well as the core of some intrinsic rotation experiments. The theory, however, is not easy to track analytically, and a detailed computational investigation is challenging. Furthermore, for the edge of the plasma the not well understood H-mode physics severely hinders the development of the theory. The way forward is undoubtedly the identification of those processes that dominate, rather than treating all possible processes. Dominant mechanisms in the edge are likely connected with the strong profile variation of density, temperature, and potential, and possibly with the change in the equilibrium close to the X-point.

## References

- [1] H. Biglari, P.H. Diamond, and P.W. Terry, Phys. Fluids B **2**, 1 (1990).
- [2] R. E. Waltz *et al.*, Phys. Plasmas **1**, 2229 (1994).
- [3] A. Bondeson *et al.*, Phys. Rev. Lett. **72**, 2709 (1994)
- [4] E.J. Strait *et al.*, Phys. Rev. Lett. **74**, 2483 (1995)
- [5] A.G. Peeters, C. Angioni, Phys. Plasmas **12**, 72515, (2005)
- [6] J.E. Kinsey, R.E. Waltz, and J. Candy, Phys. Plasmas **12**, 062302 (2005)
- [7] C.M. Roach *et al.*, Plasma Phys. Control. Fusion **51**, 124020 (2009)
- [8] S. Suckewer, *et al.*, Nucl. Fusion **21** 1301 (1981)
- [9] K. Burrell, *et al.*, Nucl. Fusion **28**, 3 (1988)
- [10] H. Weisen, *et al.*, Nucl. Fusion **29**, 2187 (1989)
- [11] S.D. Scott, *et al.*, Phys. Rev. Lett. **64**, 531 (1990)
- [12] A. Kallenbach, *et al.*, Plasma Phys. Control. Fusion **33**, 595 (1991)
- [13] N. Asakura, *et al.*, Nucl. Fusion **33**, 1165 (1993)
- [14] K. Nagashima, *et al.*, Nucl. Fusion **34**, 449 (1994)
- [15] K.D. Zastrow, *et al.*, Nucl. Fusion **38**, 257 (1998)
- [16] J.S. deGrassie, *et al.*, Nucl. Fusion **43** 142 (2003)
- [17] D. Nishijima, *et al.* Plasma Phys. Control. Fusion **47** 89 (2005)
- [18] N. Mattor, Phys. Fluids **31**, 1180 (1988)
- [19] L-G. Eriksson *et al.* Plasma Phys. Control. Fusion, **39**, 27 (1997).
- [20] J.E. Rice *et al.* Nucl. Fusion, **38**, 1 (1998).
- [21] I.H. Hutchinson *et al.* Phys. Rev. Lett., **84**, 3330 (2000).
- [22] G.T. Hoang *et al.* Nucl. Fusion, **40**, 913 (2000).
- [23] J.S. deGrassie *et al.* Phys. Plasmas, **11**, 4323 (2004).
- [24] Y. Sakamoto *et al.* Plasma Phys. Control. Fusion, **28**, A63 (2006).

- [25] A. Scarabosio et al. Plasma Phys. Control. Fusion, **48**, 663 (2006).
- [26] J.E. Rice et al. Nucl. Fusion, **47**, 1618, (2007).
- [27] J.E. Rice, et al., Nuclear Fusion **38**, 75 (1998)
- [28] F.I. Para, et al., Plasma Phys. Control. Fusion **52**, 045004 (2010)
- [29] J. Abiteboul et al., Proceedings of the 37th EPS Conference on Plasma Physics (European Physical Society Vienna) P1.1001 (2010)
- [30] P.H. Diamond, Phys. Plasmas **15**, 012303 (2008)
- [31] F. Parra et al., submitted to Phys. Plasmas (2010)
- [32] R.R. Dominguez, G.M. Staebler, Phys. Fluids B **5**, 3876 (1993).
- [33] A.G. Peeters et al., Phys. Plasmas **16**, 062311 (2009)
- [34] A.G. Peeters et al., Comp. Phys. Comm., **180**, 2650 (2009)
- [35] R.E. Waltz, et al., Phys. Plasmas **14**, 122507 (2007)
- [36] F.J. Casson, et al., Phys. Plasmas **16**, 092303 (2009)
- [37] A.R. Polevoi et al., Proc. 19th Int. Conf. on Fusion Energy (2004) (Lyon 2002) (Vienna: IAEA)
- [38] D. Strintzi, et al., Phys. Plasmas **15**, 044502 (2008)
- [39] J. Weiland et al., Nucl. Fusion **49** 065033, (2009)
- [40] A.G. Peeters et al., Plasma Phys. Contr. Fusion **48**, B413 (2006)
- [41] I. Holod, Z. Lin, Phys. Plasmas **15**, 092302 (2008)
- [42] I. Holod, Z. Lin, Plasma Phys. Contr. Fusion **52**, 035002 (2010)
- [43] W.X. Wang et al., Phys. Plasmas **17**, 072511 (2010)
- [44] A.P. Snodin, In preparation for Phys. Plasmas
- [45] A.G. Peeters, et al., Phys. Rev. Lett. **98**, 265003 (2007)
- [46] T.S. Hahm et al., Phys. Plasmas **14**, 072302 (2007)
- [47] A.G. Peeters et al., Phys. Plasmas **16**, 042310 2009
- [48] A.J. Brizard, Phys. Plasmas **2**, 459 (1995)
- [49] A.G. Peeters et al., Phys. Plasmas **16**, 034703 (2009)
- [50] T.S. Hahm, et al., Phys. Plasmas **15**, 055902 (2008)
- [51] Ö. D. Gürçan, et al., Phys. Rev. Lett. **100**, 135001 (2008)
- [52] N. Kluy, et al., Phys. Plasmas **16**, 122302 (2009)
- [53] C. Angioni, et al., Phys. Rev. Lett. **90**, 205003 (2003)
- [54] X. Garbet, et al., Phys. Rev. Lett. **91**, 035001 (2003)
- [55] C. Estrada-Mila, et al., Phys. Plasmas **13**, 074505 (2006)
- [56] C. Angioni, et al., Phys. Plasmas **16**, 060702 (2009)
- [57] X. Garbet, et al, Phys. Plasmas **9**, 3893 (2002)
- [58] Ö. D. Gürçan, et al., Phys. Plasmas **14**, 042306 (2007)
- [59] Y. Camenen, et al., Phys. Rev. Lett. **102**, 125001 (2009)
- [60] Y. Camenen, et al., Phys. Plasmas **16**, 062501 (2009)
- [61] C.J. McDevitt, et al., Phys. Rev. Lett **103**, 205003 (2009)
- [62] C.J. McDevitt et al., Phys. Plasmas **16**, 052302 (2009)
- [63] O.D. Gurcan et al., Phys. Plasmas **17**, 032509 (2010)
- [64] B.D. Scott, et al., '*Energetic Consistency and Momentum Conservation in the Gyrokinetic Description of Tokamak Plasmas*' <http://de.arxiv.org/abs/1008.1244> Submitted to Physics of plasmas.
- [65] C.J. McDevitt et al., Phys. Plasmas **16**, 012301 (2009)
- [66] P.H. Diamond et al., Nucl. Fusion **49**, 045002 (2009)